AMEGHINIANA
A GONDWANAN PALEONTOLOGICAL JOURNAL

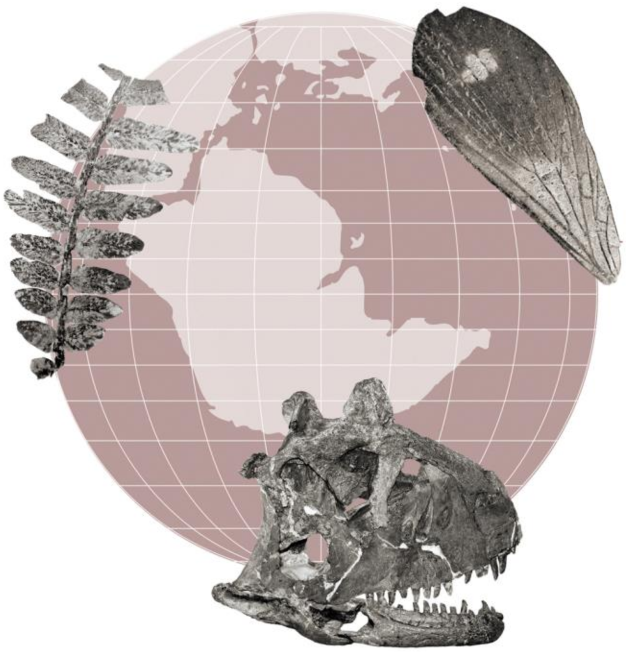

Submitted: 31 July 2024 - **Accepted**: 22 May 2025 - **Posted online**: 5 September 2025

To link and cite this article:

doi: 10.5710/AMGH.22.05.2025.3620

THE INFRAORBITAL FORAMEN IN SPARASSODONTA (MAMMALIA, METATHERIA), EXTINCT NATIVE PREDATORS OF SOUTH AMERICA

CATALINA SUAREZ[1], CHARLÈNE GAILLARD[1], ROSS D.E. MACPHEE[2], AND ANALÍA M. FORASIEPI[1]

[1]Instituto Argentino de Nivología, Glaciología y Ciencias Ambientales (IANIGLA), CCT-CONICET Mendoza, Av. Ruiz Leal s/n°, Parque General San Martín, 5500, Mendoza, Argentina. catasuarezg@gmail.com; charlene.gaillard.pal@gmail.com; acanthodes@gmail.com

[2]Division of Vertebrate Zoology, Department of Mammalogy, American Museum of Natural History, 200 Central Park West, 10024-5102, New York, U.S.A. macphee@amnh.org

22 pag.; 3 figs.; 1 table

Running Header: SUAREZ *ET AL.*: INFRAORBITAL FORAMEN IN SPARASSODONTA

Short Description: This study investigates the infraorbital foramen (IOF) size and its implications for the paleoecology of sparassodonts, focusing on *Thylacosmilus*.

Corresponding author: Catalina Suarez, catasuarezg@gmail.com

Abstract. The Sparassodonta were the dominant mammalian predators in South America during much of the Cenozoic. Among them, *Thylacosmilus atrox*, with its hyperdeveloped upper canines and bizarre anatomy, has drawn considerable attention. This study investigates infraorbital foramen (IOF) size and its implications for the paleoecology of sparassodonts, focusing on *Thylacosmilus*. Using computed tomography (CT), micro-computed tomography (μCT), and comparative analyses, we examined the relationship between IOF area (IOF_{area}) and certain anatomical correlates, including foramen rotundum area (FR_{area}), several endocranial structures, and skull dimensions. Comparisons were made within Sparassodonta and to marsupials and carnivorans. Our results reveal that greater variation in IOF_{area} exists among sparassodonts compared to marsupials, with some large borhyaenoids exhibiting disproportionally large IOF_{area}. Notably, *Thylacosmilus* displays intrataxon variation in IOF_{area}. Contrary to previous studies, which concluded that *Thylacosmilus* possessed a relatively small IOF that might have been consistent with scavenging behavior, our findings indicate that IOF_{area} in *Thylacosmilus* does not substantially differ from that of the active predators in our sample. This study highlights the anatomical diversity of IOF in sparassodonts and underscores the complexity of making behavioral inferences from partial cranial morphology.

Keywords. Maxillary nerve. Infraorbital nerve. Foramen rotundum. *Thylacosmilus*.

Resumen. EL FORAMEN INFRAORBITARIO EN SPARASSODONTA (MAMMALIA, METATHERIA), LOS DEPREDADORES NATIVOS SUDAMERICANOS. Los Sparassodonta fueron los principales mamíferos depredadores de América del Sur durante el Cenozoico. Entre ellos, *Thylacosmilus atrox*, con sus caninos superiores hiperdesarrollados y su peculiar anatomía, ha atraído considerable la atención. Este estudio investiga el tamaño del foramen infraorbitario

(IOF) y sus implicancias para la paleoecología de los Sparassodonta y en particular *Thylacosmilus*. Utilizando tomografías computarizadas (CT) y micro-tomografías computarizadas (μCT), así como análisis comparativos, se examinó la relación entre el área del IOF (IOF_{area}) y aspectos anatómicos como el área del foramen rotundum (FR_{area}), algunas estructuras endocraneales y las dimensiones del cráneo en varios Sparassodonta, comparándolos con marsupiales y carnívoros. Nuestros resultados revelan una mayor variabilidad en la IOF_{area} entre los esparasodontes en comparación con los marsupiales, con algunos grandes borhyaenoides presentando un área desproporcionalmente grande. Notablemente, *Thylacosmilus* muestra una variación del IOF_{area} entre individuos. En contraste con previos estudios que afirmaban que *Thylacosmilus* poseía un IOF relativamente pequeño que implicaría un comportamiento carroñero, nuestros hallazgos indican que el IOF de *Thylacosmilus* no difiere sustancialmente del de los depredadores activos de nuestra muestra. Este estudio resalta la diversidad anatómica del IOF de los Sparassodonta y la complejidad de realizar inferencias paleoecológicas a partir del análisis parcial de la morfología craneal.

Palabras clave. Nervio maxilar. Nervio infraorbitario. Foramen rotundum. *Thylacosmilus*.

Sparassodonta (Mammalia, Metatheria), a wholly extinct clade of South American metatherians, were the only mammalian predators on that continent for most of the Cenozoic. Although sparassodonts were a diverse group, the taxon that has received the most attention is *Thylacosmilus atrox,* sometimes called the “marsupial saber-tooth” in reference to its extremely hypertrophied maxillary canines. Previous authors have recognized notable variation among specimens of *Thylacosmilus*, and we follow Goin & Pascual (1987) in recognizing a single, highly variable species. In the absence of any obvious extant ecological analogues, making inferences about its paleoecology has proven difficult (see Riggs, 1934; Marshall, 1976; Wroe *et al.*, 2013; Janis *et al.*, 2020; Suarez *et al.*, 2023; Wroe & Sansalone, 2023). Although its dental battery as a whole suggests hypercarnivory (e.g., great reduction of the protocone, talonid basin, participants in the crushing mechanism; and a strong development of cutting blades: preparacrista, postmetacrista, and paracristid), it has recently been questioned whether it was an active predator, as opposed to a scavenger, given its supposedly “relatively small” infraorbital foramen (IOF), among other features (Janis *et al.*, 2020; Janis, 2024; but see Discussion). A “relatively small” IOF was thought to imply a “lesser amount of sensory feedback from the muzzle and, hence, lesser ability for precise positioning of the canine” (Janis, 2024: 9).

Most cranial apertures are multipurpose, providing ingress/egress for both nerves and the blood vascular system. How much of a foramen’s cross-sectional area is devoted to the passage of soft tissues may vary considerably across taxa, making it difficult to make functional inferences alone. In the case of the IOF, however, available comparative evidence indicates that its primary component is always nervous, occupying as much as 80–90% of the cross-sectional area of the foramen (IOF_{area}; Sánchez-Villagra & Asher, 2002; Wible, 2003; Muchlinski, 2008; Evans & Lahunta, 2012). The vascular component, if any, is usually quite small. The infraorbital nerve (ION) is a branch of the maxillary nerve, which leaves the cranial cavity via the foramen rotundum (FR; if present as a separate foramen). The ION's general sensory field is the middle of the face, which includes the muzzle, and any specialized external structures connected with it, such as vibrissae. As vibrissae relay tactile information concerning the environment, head position, obstacles and so forth, it is reasonable to ask whether IOF_{area} is correlated with the amount of sensory information an animal receives along this pathway.

Previous analyses have focused on normalizing IOF size to the general size of the skull, as a way of indexing the relationship of IOF_{area} to vibrissae number or proportion. Translating that information into inferences about behavior or ecology is largely based on conditions in eutherians (e.g., Luo, 2007; Muchlinski, 2010a,b; Wilson *et al.*, 2012; Gill *et al.*, 2014; Muchlinski *et al.*, 2020). Little attention has been given to marsupials, the metatherian crown group (but see Muchlinski, 2010b), and apart from brief comments on some groups (e.g., Engelman & Croft, 2014; Janis *et al*., 2020; Janis, 2024), IOF morphology has not been studied in detail for this clade.

Using μCT it is possible to make wide anatomical analyses, such as comparing IOF_{area} to portions of the brain (as visualized from endocast reconstructions) involved with vision, audition, and olfaction (e.g., Gaillard *et al*., 2021, 2023, 2024). By focusing on *Thylacosmilus* and its close relatives, we explore inter- and intra-specific variability of IOF_{area} in sparassodonts in relation to skull dimensions and specific areas of the brain. Here we make comparisons to their closest extant relatives (marsupials) and plausible ecological analogues (carnivorans) to elucidate the possible role(s) of IOF contents. One hypothesis of interest in this regard is the metrical relationship between IOF_{area} and foramen rotundum area (FR_{area}), which we explore in some detail.

Institutional abbreviations. **AMNH VP**, Department of Vertebrate Paleontology, American Museum of Natural History, New York, USA; **CORD-PZ**, Museo de Paleontología, Facultad de Ciencias Exactas, Físicas y Naturales de la Universidad Nacional de Córdoba, Córdoba, Argentina; **FMNH P**, Field Museum of Natural History, Paleontological collection, Chicago, USA; **MACN**, Museo Argentino de Ciencias Naturales 'Bernardino Rivadavia' (MACN-A, Ameghino collection; MACN-Ma, Mammal collection; MACN-Pv CH, Paleovertebrados, Chubut collection), Ciudad Autónoma de Buenos Aires, Argentina; **MCNAM-PV**, Colección de Paleontología de Vertebrados, Museo de Ciencias Naturales y Antropológicas Juan Cornelio Moyano, Mendoza, Argentina; **MLP-PV**, Colección de Paleontología de Vertebrados, Museo de La Plata, La Plata, Argentina; **MMP**, Museo Municipal de Ciencias Naturales de Mar del Plata "Lorenzo Scaglia", Mar del Plata, Argentina; **MPM-PV**, Colección de Paleontología de Vertebrados, Museo Regional Provincial "Padre M. J. Molina", Río Gallegos, Argentina; **NMB**, Naturhistorisches Museum Basel, Basel, Switzerland; **PVL**, Paleontología de Vertebrados Lillo, Facultad de Ciencias Naturales e Instituto Miguel Lillo, San Miguel de Tucumán, Argentina; **TMM-M**, Texas Memorial Museum, Mammal collection, Austin, USA; **YPM-VPPU**, Princeton University collection, Yale Peabody Museum of Natural History, New Haven, USA.

Anatomical abbreviations. C/c, upper/lower canines; **FR**, foramen rotundum; I/i, upper/lower incisors; **IOF**, infraorbital foramen; **ION**, infraorbital nerve; **M/m,** upper/lower molars; P/p, upper/lower premolars.

Other abbreviations. **BM**, body mass; **CS**, cranium size (i.e., geometric mean of cranial shape in Muchlinski, 2010a,b); **CT**, computed tomography; **µCT**, micro-computed tomography; **LDA**, Linear Discriminant Analysis; **ln**, natural logarithm;

PCA, Principal Component Analysis; R^2, coefficient of determination; **S1–3**, Supplementary Online Information table 1–3; **SE**, Smearing Estimate.

Dental formula. The conventional primitive metatherian dental formula followed in this contribution is: I 1–5 / i 2–5, C/c 1, P/p 1–3, M/m 1–4 (e.g., see Voss & Jansa, 2009; Goin *et al.*, 2016; Beck *et al.*, 2022, and literature cited). For postcanine homology considering ontogeny and character evolution in high-level mammalian phylogeny see for example Luckett (1993) and O'Leary *et al.* (2013).

MATERIAL AND METHODS

Material

Table 1 lists the sparassodont specimens that are our primary focus and certain marsupials included to provide a phylogenetic framework. Comparative information on other metatherians, placental carnivorans, and primates taken from the literature (Muchlinski, 2010a,b) is provided in Tables S2–3.

Analyses comparing IOF_{area} with FR_{area}, olfactory bulbs, and orbital convergence are based on tomographic measurements collected from our specimens set (Table 1).

Methods

Image processing and measurements. Specimens were studied via CT and μCT scans. Scanning parameters and related data are given in Table S1 for each examined specimen. CT scans were initially processed in the open software Image J (Schneider *et al.*, 2012) to enhance contrast and reduce file size. Tridimensional models were generated by segmentation using the software Avizo/Amira (Zuse Institute Berlin and Visualization Sciences Group, 1995–2012) and the open software 3D Slicer (Fedorov *et al.*, 2012). Linear measurements of the skull were taken on CT scans using 3D Slicer v. 5.2.2 for Linux. Measurements of the IOF_{area} and FR_{area} were taken directly in 3D Slicer using the Markups module (Fig. 1). To accomplish this, orthogonal CT sections were reoriented as follows: the axial and sagittal planes were oriented parallel to the canal, and the coronal plane was oriented perpendicular to them (Fig. 1.1–1.3). A closed curve was drawn along the margin of the foramen on the coronal slice so that the area enclosed would be transverse to the canal (Fig. 1.1, 1.4–1.5). The area surrounded by that curvature, corresponding to the foramen area, was calculated by the software. These measurements correspond to those presented by Muchlinski *et al.* (2020) with the difference that those authors used latex casts instead of virtual 3D meshes of the canals. In some specimens, the borders of the FR or IOF were incomplete due to breakage. In those cases, we measured the rostralmost portion of their preserved transverse areas. Linear cranial length and bizygomatic width measurements follow Muchlinski (2010a,b).

Figure 1 here

Most of the specimens in our sample have a single aperture of IOF. However, in specimen NMB c.2526 of *Thylacinus cynocephalus*, we detected multiple apertures of IOF. For our analysis, we summed the individual apertures into a total area. Regarding Sparassodonta, accessory foramina around IOF were observed in specimen YPM-VPPU 15701 of *Borhyaena tuberata* (Sinclair, 1906; not included in our sample set). In the absence of CT, it is unclear if both openings are for the ION (i.e., in this case, we would expect that both facial openings connect with the maxillary canal) or if at least one of the openings is for vasculature only (e.g., diploic or emissary foramina, justifying excluding it from the analysis). In addition, by surface inspection Babot *et al*. (2002) mentioned that specimen PVL 4187 of *Callistoe vincei* exhibits multiple apertures of

IOF. However, CT scanning reveals that two accessory foramina appear only on the right side of the cranium, and directly lead to the alveolar space of P3 without connecting to the maxillary canal. We interpret that their content was most likely vascular and/or indirectly related to the ION (e.g., superior alveolar nerve and vessels) and consequently excluded from our measurement of the IOF_{area}.

The measurements taken in this study are given in Table 1. The complete dataset of measurements compiled from Muchlinski (2010a,b) and additional estimations made in the present study are provided in Tables S2–3. The angles of orbital convergence and olfactory bulb percentages were taken from Gaillard *et al.* (2023, 2024) and Gaillard (2024).

Analyses. In our initial analyses we explored several datasets and variables not only using bivariate plots but also PCA and LDA, to ensure a consistent analytical approach across datasets with varying numbers of variables. Even when we retained for discussion those analyses with only two variables (as ones we considered the most informative; Fig 2), we decided to show their PCA and LDA results in the Supplementary Online Information Figures (Figs. S2–3), as these approaches allowed to visualize the data in a transformed space more clearly than in a biplot (e.g., visualize the different groups and their overlaps). While bivariate plots effectively illustrate direct relationships, PCA and LDA provide standardized, orthogonal axes that can reveal underlying patterns and maximize group separation, respectively. This multivariate approach facilitates direct comparison of results across all analyses and helps to identify features that may not be immediately apparent from raw variable plots alone (Jolliffe & Cadima, 2016; James *et al*., 2021; Greenacre *et al*., 2022).

Bivariate regression analyses (XY plots) were conducted in Microsoft Excel. Exploratory analyses, including PCA and LDA, were made using the open software

PAST (Hammer *et al.*, 2021). The IOF_{area} was examined in comparison to the general cranium size (CS), using the geometric mean of cranial shape (calculated based on cranial length and maximum bizygomatic width) as body size correction, following Muchlinski (2010b).

Dataset 1 (i.e., Sparassodonta, Marsupialia, and Carnivora; Tables 1, S2) was used to compare the ln(IOFarea) and ln(CS) in an XY plot (Fig. 2.1; S1). We also made exploratory analyses with this dataset (Figs. S2–3; Tables S4–5).

Dataset 2 (i.e., Sparassodonta and Marsupialia variables measured from CT scans, plus Primates sample from Muchlinski, 2010a; see Tables 1, S3) was used to test differences among body size correction parameters. We compared the ln(IOF_{area}) with the ln(CS) and ln(BM) using XY plots (Figs. S4–5). Primates were included to leverage the extensive dataset from Muchlinski (2010a) for this comparison. BM estimations (Table 1) for non-borhyaenoid sparassodonts (when possible, excepting one incomplete specimen of *Cladosictis patagonica*) were made based on M2 length, following Zimicz (2012). For borhyaenoids, we used orbital-occiput length (OOL; when possible, excepting incomplete *Patagosmilus goini*), following Van Valkenburgh (1990), to avoid underestimation produced by dental variables (see Prevosti *et al.*, 2012).

We hypothesized that enhancement in other sensory areas of the head could compensate for a diminution in certain sensory capabilities. Dataset 3 (i.e., Sparassodonta and Marsupialia measured from CT scans; see Table 1) was used to contrast the “relative” IOF_{area} (following Muchlinski, 2010b) with other measurable parameters related to other cranial sensory areas (Table S1): the percentage of braincase endocast volume filled by the olfactory bulbs (Macrini, 2006; Macrini *et al.*, 2007; Fig. S6) and the angle of orbital convergence (Gaillard *et al.*, 2023; Fig. S7). In the two lastnamed analyses, we did not separately discriminate specimens but instead used average data for each species.

The last parameter to be evaluated was FR_{area}, selected because of the anatomical relationship between it and the distal part of the maxillary nerve (aperture to IOF). We compared the relation between the ln(FR_{area}) and the ln(CS) (Fig. 2.2), and between the ln(IOF_{area}) and ln(FR_{area}; Fig. 2.3), using Dataset 3. Additionally, we calculated the ratio between the FR_{area} and IOF_{area}, to obtain a measurable index to express the differences in these areas (Table 1). The closer the index to 1, the more similar the areas. The lowest values show the largest area difference, meaning a relatively larger IOF.

RESULTS

We compared body size correction parameters (CS and BM) and found no considerable differences in our results (Figs. S4–5). However, since BM estimation is particularly challenging for groups like sparassodonts, which lack extant representatives (e.g., Nelson *et al*., 2024), we focused here on the results obtained using the CS (i.e., geometric mean in Muchlinsky, 2010a,b) as a proxy for body size.

With some exceptions (see below), marsupials display a consistent relationship between IOF_{area} and CS, as IOF_{area} is proportionally similar across the entire size spectrum of species in our marsupial sample (Fig. 2.1). However, among marsupials, *Thylacinus cynocephalus* has an IOF_{area} relatively larger than that of other members of this group (including dasyurids) and plots near sparassodonts. Among sparassodonts, there are some species in which the IOF_{area} is proportionally larger than expected for their CS (e.g., *Arctodictis, Borhyaena*, *Callistoe,* and *Thylacosmilus* compared to *Cladosictis*; Fig. 2.1).

Figure 2 here

Specimen MPM-PV 3625 of *Borhyaena tuberata* does not closely group with other specimens of this species. This may be an artefact, as this specimen was analyzed with a medical scanner, which potentially affects the precision of measurements. For this reason, we focus on other specimens of this species (YPM-VPPU 15120, digitalized with μCT; and MPM-PV 4380, with results congruent with the YPM specimen).

Contrasting the IOF_{area} and the CS, sparassodonts partially overlap with marsupials and completely plot inside the range of variation found in carnivorans (Figs. 2.1, S1). Compared to other taxa, sparassodonts show a more pronounced positive allometry in IOF size, as indicated by the more positive slope of the regression line (Fig. 2.1). This result is probably a consequence of differences in IOF size between borhyaenoids and hathliacynids. Additionally, the exploratory analyses show a slight predominance of the $\ln(IOF_{area})$ variable in the PCA (Fig. S1), with sparassodonts closer to this variable than to the ln(CS). This is even more evident in the LDA (Fig. S2) where the $\ln(IOF_{area})$ discriminant is more dominant and the sparassodont species are much closer to each other. These results imply that the IOF_{area} is not entirely proportional to total skull size but tends to be disproportionally bigger in larger sparassodonts.

Among sparassodonts, contrasting results were observed for small (hathliacynids) vs. large (borhyaenoids) species in our sample. Borhyaenoids show relatively larger IOF than hathliacynids. Within Hathliacynidae, there is comparably little intraspecific variation in IOF_{area} relative to the CS compared to Borhyaenoidea (Fig. 2.1). Among Borhyaenoidea there is not a close grouping graphically among specimens of the same species nor a clear pattern of relationship between the evaluated parameters (Fig. 2). From our analyses we highlight two main results: (1) large borhyaenoids such as *Arctodictis sinclairi*, *A. munizi*, *Borhyaena tuberata*, *Callistoe vincei*, and *Thylacosmilus atrox* have proportionally larger IOF_{area}; and (2) in *Thylacosmilus atrox*, IOF_{area} varies among different individuals of the same species (Table 1; Fig. 2).

Another relationship of interest is relative IOF_{area} plotted against relative volume of the olfactory bulbs (Fig. S6). Mammals with larger olfactory bulbs relative to total braincase endocast volume have demonstrably better olfactory capabilities than mammals with smaller bulbs (e.g., Gittelman, 1991). Given this relationship, we expected that sparassodont species with smaller olfactory bulbs would have less developed olfactory capabilities, raising the possibility that other sensory modalities, such as those innervated by the ION, might have been enhanced. However, no clear pattern of enhancement in the form of a larger relative IOF_{area} compared to olfactory bulbs was found (Fig. S7).

When relative IOF_{area} is plotted against the angle of orbital convergence (Fig. S7) we observe that, for all sparassodonts and marsupials with larger infraorbital foramina, there is a similar pattern of having smaller angles of orbital convergence. We recognize the difficulty and uncertainty of recovering a true pattern using our small sample size. However, assuming that a similar result could be obtained with a larger sample, this might indicate some relationship between the organization of the orbits and the sensitivity of the snout in metatherians, where the role of specialized organs like the vibrissae or rhinarium is enhanced when 3D vision is limited.

Evaluating the variability of the IOF_{area} compared to the FR_{area}, we observe four main results: (1) sparassodonts have a proportionally larger FR_{area} compared to other metatherians (Fig. 2.2); (2) sparassodonts have a higher dispersion in their FR_{area} values, compared to the CS (Fig. 2.2) and IOF_{area} (Fig. 2.3); (3) the relationship between IOF_{area} and FR_{area} remains relatively more constant in hathliacynids than in most analyzed borhyaenoids; and (4), some borhyaenoids (i.e., *Arctodictis sinclairi*, *A. munizi*, *Borhyaena tuberata*, *Prothylacynus patagonicus*, and the specimen FMNH P14531 of *Thylacosmilus atrox*—but not MMP 1443-M and MLP-PV 35-X-4-1—; see discussion) have disproportionally larger IOF relative to the FR. These observations are supported by a lower index FR_{area}/ IOF_{area} (values lower than 0.35; Table 1). Hathliacynids are within the range of the marsupials evaluated (FR_{area}/ IOF_{area} values higher than 0.35).

DISCUSSION

Despite the limitations of small sample size, sparassodonts display more variation overall than extant marsupials. Some taxa with disproportionally large IOF size compared to CS (e.g., *Arctodictis, Borhyaena, Callistoe*, some specimens of *Thylacosmilus*) are more similar to carnivorans than to marsupials (Fig. 2.1).

Among extant species, placental mammals with a short snout usually have a smaller IOF (Kästner, 2014; Davis *et al.*, 2021). However, this pattern is not evident in sparassodonts, as borhyaenoids (e.g., *Arctodictis, Borhyaena)* with shorter snouts have a relatively larger IOF compared to hathliacynids (e.g., *Cladosictis*) with longer snouts and smaller IOF_{area}. Additionally, in some of the sparassodonts studied, such as *Thylacosmilus atrox*, IOF_{area} shows the largest variation encountered in our mammal sample. This result is consistent with the degree of anatomical variability of this species reported previously (see Riggs, 1934; Goin & Pascual, 1987; Marshall, 1976).

Some previous studies considered that *Thylacosmilus* had a relatively small infraorbital foramen (Janis *et al.*, 2020; Janis, 2024). However, we found that, although the IOF_{area} of *Thylacosmilus atrox* is smaller than in the largest felids (including saber-tooth cats, such as *Smilodon populator*—with a relative IOF_{area} of 1.57 vs. 1.06 in *T. atrox*; Figs. 2, 3), it is larger than in several other felids and carnivorans with a similar CS, and is among the largest within our metatherian sample (Fig. 2). According to Janis (2024) the "small infraorbital foramen and the "virtual lack" of incisors" are characteristic of scavengers rather than active predators. The author links the small IOF_{area} of *Thylacosmilus* to a "lesser amount of sensory feedback from the muzzle and, hence, lesser ability for precise positioning of the canine". This correlation is controversial because no studies are showing a direct correlation between the size of IOF_{area} and the efficiency of ION sensory fibers with regard to canine positioning. The ION receives sensory information not only from the canine but also from the skin and mucous membranes around the middle of the face (Evans & Lahunta, 2012; Standring, 2016) including the maxillary region and rhinarium (Patrizi & Munger, 1966; Gasser & Miller Wise, 1972; Muchlinski, 2008, 2010a). Additionally, as seen in our results (Fig. 2), several extant active predators (e.g., *Felis chaus*, *F. pardalis*, *F. silvestris*, *Lynx canadensis*, *Puma concolor*) have IOF_{area} measurements that are even smaller than those of *Thylacosmilus*. In addition, sparassodonts with a bone-breaker morphology (typical of scavengers, e.g., borhyaenids; Zimicz, 2012) have an IOF_{area} larger than in *Thylacosmilus*, whether comparison of this area is made to the FR or the CS. It is also important to note that at least one pair of lower incisors has been previously reported for *Thylacosmilus* (Goin and Pascual, 1987). They are smaller than in other borhyaenoids, but the evidence is insufficient to determine whether a reduction in incisor number had actually occurred (more than one pair may have been present according to Goin & Pascual, 1987). In any case, a reduction in this part of the dentition is not characteristic of mammalian scavengers, obligate (e.g., Rieger, 1981) or facultative (e.g., Bekoff, 1977; Moehlman & Hayssen, 2018; Hayssen & Noonan, 2021). Janis (2024) concludes that *Thylacosmilus* probably does not qualify as a strict ecological analog of saber-tooth felids, and that its predatory behavior would not be the same, despite prior studies describing their broad similarities in their overall morphology and function (e.g., Wroe *et al*., 2013, Melchiona *et al*., 2021). At the same time, we agree with Janis (2024) that, in light of the unique anatomy of *Thylacosmilus*, finding analogies is probably not straightforward.

Figure 3 here

Recent studies (e.g., Muchlinski, 2010a,b; Mitchinson *et al.*, 2011; Muchlinski *et al.*, 2020; Milne *et al*., 2021; contrary to Kay & Cartmill, 1977; Muchlinski, 2008) have concluded that it is not currently possible to reconstruct vibrissal patterns or coverage—or, for that matter, any soft-tissued rhinarial or facial structure—in a completely extinct group. However, deserving of some attention is the relative size relationship between the IOF_{area} and the FR_{area} among sparassodonts, where the IOF is seen to be disproportionally large in the larger borhyaenoids sampled here (i.e., *Arctodictis munizi, A. sinclairi, Borhyaena tuberata*, *Prothylacynus patagonicus*, and the holotype of *Thylacosmilus atrox*; Fig. 2.2–2.3; see Table 1, with FR_{area}/ IOF_{area} relationship lower than 0.35). This list also includes the recently extinct marsupial wolf *Thylacinus cynocephalus* and the extant semi-aquatic didelphid *Chironectes minimus* (Table 1). In the particular case of *Thylacosmilus*, we found that the relationship between the IOF and FR varies among the different specimens evaluated (which is consistent with the known large morphological variation of this taxon). Following this index, the largest contrast between IOF and FR is found in the holotype (FMNH

P14531), while in the remaining specimens, the index is similar to that of the extant active predator *Dasyurus hallucatus*.

The infraorbital canal in mammals is occupied by the infraorbital nerve and vascular components (Sánchez-Villagra & Asher, 2002; Muchlinski, 2008), the infraorbital artery and vein. As the FR transmits the maxillary division of the trigeminal nerve (cranial nerve V), we would expect that the difference between FR and IOF areas would be more or less constant among the species evaluated if the IOF nerve bundle size remained proportionally the same. The marked difference in FR and IOF areas, as seen particularly in larger borhyaenoids, may imply that other occupants of the infraorbital canal (i.e., blood vessels) varied in ways that cannot be predicted from currently available indicia. In short, the size of IOF in these taxa does not directly reflect nerve size and/or enhanced facial sensation.

CONCLUSIONS

The relative area of the IOF in sparassodonts exhibits a broad range of variation, overlapping with data for carnivorans and large marsupials. Notably, taxa such as *Arctodictis*, *Borhyaena*, *Callistoe*, and some specimens of *Thylacosmilus* have a disproportionately large IOF_{area} relative to their skull size, resembling in this regard carnivorans more than marsupials. *Thylacosmilus atrox* shows intraspecific variation in IOF_{area}. In addition, its IOF_{area} is comparable to that of some of the active predators included in our analysis, challenging the idea that its IOF_{area} can be correlated with scavenging behavior.

The most interesting pattern we observed among sparassodonts is the relationship between IOF_{area} relative to FR_{area} (Fig. 2.3), with the IOF disproportionally larger in the largest borhyaenoids sampled. Smaller sparassodonts (hathliacynids) follow the same regression line as extant marsupials. Looking at the residuals of the relationship, hathliacynids show IOF larger than the average marsupial, but in the same general range as dasyurid marsupials (i.e., extant analogues in a roughly comparable niche). We interpret this to imply that the structure of their facial sensory areas would have been closely comparable to that of extant taxa. However, because of the lack of any relationship between the sensory areas analyzed in this study and foramina sizes in large borhyaenoids (*Arctodictis munizi*, *A. sinclairi*, *Borhyaena tuberata*, and *Thylacosmilus atrox*), we suggest that intraclade difference between small and large taxa is probably due to the presence and size of IOF vasculature.

The use of μCT scans and advanced software for 3D modeling offers a comprehensive method for studying functionally important cranial apertures. At the same time, this study highlights the complexity of interpreting the paleobiology of extinct species and emphasizes the need for multifaceted approaches in paleontological research.

ACKNOWLEDGMENTS

We acknowledge M. Sánchez-Villagra and F. J. Prevosti for valuable comments on previous versions of this manuscript. We thank Vera Weisbecker for rich discussions about *Thylacinus* IOF morphology. We thank curators who permitted the study and scanning of specimens under their care A. Kramarz, S. Alvarez, L. Chornogubsky (former), and A. Martinelli (MACN-Pv), P. Teta (MACN-Ma), M. Taglioretti and F. Scaglia (MMP), M. Reguero (MLP), D. Brinkman (YPM), R. O'Leary and J. Galkin (AMNH), G. Campos (MCNAM), as well as S. F. Vizcaino, S. Bargo (MLP), and E. Cerdeño (IANIGLA) for granting access to sparassodonts specimen from their recent excavations housed at MPM and MCNAM, respectively. We thank F. J. Prevosti

(Museo de Ciencias Antropológicas y Naturales de la Universidad Nacional de La Rioja), L. Costeur (NMB), G. Schultz (Biomaterial Science Center), S. Ladevèze (Musée National d'Histoire Naturelle), Marta Bellato (AST-RX, Project ASTRX-2015-022), Zhe-Xi Luo (University of Chicago), L. Witmer (Ohio University), M. Taglioretti and F. Scaglia (MMP), the Instituto Radiólogico Mar del Plata (Iradiologico), Judith Babot (Fundación Miguel Lillo), C. Capiel, and S. Rossini (Iradiologico), the Facultad de Matemática, Astronomía, Física y Computación (FAMAF), G. Tirao (FAMAF), the Clínica La Sagrada Familia, the Equipo de Neurocirurgía Endovascular Radiología Intervencionista (ENERI) and the Fundación Escuela de Medicina Nucelar (FUESMEN), and Diagnósticos Gamma, Tucumán, for their help with the tomographies. For data accessibility, we would like to acknowledge DigiMorph.org, The University of Texas High-Resolution Xray CT Facility (UTCT) (Dr. Ted Macrini, NSF grants IIS-0208675 and DEB-0309369); and Morphosource.org, Duke University (Eric Delson and the AMNH Department of Mammalogy, collection funded by AMNH and NYCEP). This research was partially funded by the projects PICT 2019-2874 and SNF-SPIRIT, IZSTZ0-208545. We thank Russell Engelman, the anonymous reviewer, and editor Darin Croft for their valuable comments and suggestions, which enhanced the quality of this manuscript.

REFERENCES

Beck, R. M., Voss, R. S., & Jansa, S. A. (2022). Craniodental morphology and phylogeny of marsupials. *Bulletin of the American Museum of Natural History, 457*(1), 1–352.

Bekoff, M. (1977). *Canis latrans*. *Mammalian Species, 79,* 1–9. https://doi.org/10.2307/3503817

Davis, L. V., Hoyer, N. K., Boscan, P., Rao, S., & Rawlinson, J. E. (2021). Computed tomography analysis of the feline infraorbital foramen and canal. *Frontiers in Veterinary Science, 7*(619248), 1–6. https://doi.org/10.3389/fvets.2020.619248

Engelman, R. K., & Croft, D. A. (2014). A new species of small-bodied sparassodont (Mammalia, Metatheria) from the Middle Miocene locality of Quebrada Honda, Bolivia. *Journal of Vertebrate Paleontology*, *34*(3), 672–688. http://dx.doi.org/10.1080/02724634.2013.827118

Evans, H. E., & Lahunta, A. de. (2012). *Miller's anatomy of the dog* (4th ed.). Elsevier Health Sciences.

Fedorov, A., Beichel, R., Kalpathy-Cramer, J., Finet, J., Fillion-Robin, J.-C., Pujol, S., Bauer, C., Jennings, D., Fennessy, F., Sonka, M., Buatti, J., Aylward, S., Miller, J. V., Pieper, S., & Kikinis, R. (2012). 3D Slicer as an image computing platform for the Quantitative Imaging Network. *Magnetic Resonance Imaging, 30*(9), 1323–1341. https://doi.org/10.1016/j.mri.2012.05.001

Forasiepi, A. M. & Sánchez Villagra, M. R. (2014). Heterochrony, dental ontogenetic diversity and the circumvention of constraints in marsupial mammals and extinct relatives. *Paleobiology, 40*, 222–237.

Gaillard, C. (2024). Evolución de las estructuras encefálicas de los mamíferos depredadores nativos de América del Sur, su relevancia para inferir hábitos paleoecológicos y el rol de los Sparassodonta en los ecosistemas del Cenozoico (Tesis Doctoral, Programa de Postgrado en Biología, Universidad Nacional de Cuyo, Mendoza).

Gaillard, C., Forasiepi, A. M., S. D., MacPhee, R. D. E., & Ladevèze S. (2024). Cranium of *Sipalocyon externus* (Metatheria, Sparassodonta) with remarks on the paleoneurology of hathliacynids and insights into the Early Miocene sparassodonts of Patagonia, Argentina. *Swiss Journal of Palaeontology, 143*(20), 1–34. https://doi.org/10.1186/s13358-024-00312-x

Gaillard, C., MacPhee, R. D. E., & Forasiepi, A. M. (2021). The stapes of stem and extinct Marsupialia: Implications for the ancestral condition. *Journal of Vertebrate Paleontology, 41*(2), e1924761. https://doi.org/10.1080/02724634.2021.1924761

Gaillard, C., MacPhee, R. D. E., & Forasiepi, A. M. (2023). Seeing through the eyes of the sabertooth *Thylacosmilus atrox* (Metatheria, Sparassodonta). *Communications Biology*, *6*(257), 1–7. https://doi.org/10.1038/s42003-023-04624-5

Gasser, R. F., & Miller Wise, D. (1972). The trigeminal nerve in the baboon. *The Anatomical Record*, *172*(3), 511–522. https://doi.org/10.1002/ar.1091720305

Gill, P. G., Purnell, M. A., Crumpton, N., Brown, K. R., Gostling, N. J., Stampanoni, M., & Rayfield, E. J. (2014). Dietary specializations and diversity in feeding ecology of the earliest stem mammals. *Nature, 512*(7514), 303–305. https://doi.org/10.1038/nature13622

Goin, F. J., & Pascual, R. (1987). News on the biology and taxonomy of the marsupials Thylacosmilidae (late Tertiary of Argentina). *Anales de La Academia Nacional de Ciencias Exactas, Físicas y Naturales (Argentina), 39*, 219–246.

Goin, F.J., Woodburne, M.O., Zimicz, A.N., Martin, G.M., & Chornogubsky, L. (2016). *A brief history of South American metatherians. Evolutionary contexts and intercontinental dispersals*. Springer. http://dx.doi.org/10.1007/978-94-017-7420-8

Greenacre, M., Groenen, P. J., Hastie, T., D'Enza, A. I., Markos, A., & Tuzhilina, E. (2022). Principal component analysis. *Nature Reviews Methods Primers, 2,* 100. https://doi.org/10.1038/s43586-022-00159-0

Hammer, Ø., Harper, D. A. T., & Ryan, P. D. (2001). PAST: Paleontological statistics software package for education and data analysis. *Palaeontologia Electronica, 4*(1), 1–9. http://palaeo-electronica.org/2001_1/past/issue1_01.htm.

Hayssen, V., & Noonan, P. (2021). *Crocuta crocuta* (Carnivora: Hyaenidae). *Mammalian Species, 53*(1000), 1–22. https://doi.org/10.1093/mspecies/seab002

Hiatt, J. L., & Gartner, L. P. (1987). *Textbook of head and neck anatomy* (2nd ed.). Lippincott Williams and Wilkins.

Horn, R. N. V. (1970). Vibrissae structure in the *Rhesus* monkey. *Folia Primatologica, 13*(4), 241–285. https://doi.org/10.1159/000155325

James, G., Witten, D., Hastie, T., & Tibshirani, R. (2021). *An Introduction to Statistical Learning: with Applications in R* (2nd ed.). Springer.

Janis, C. M. (2024). Who was the real sabertooth predator: *Thylacosmilus* or *Thylacoleo*? *The Anatomical Record*. https://doi.org/10.1002/ar.25444

Janis, C. M., Figueirido, B., DeSantis, L., & Lautenschlager, S. (2020). An eye for a tooth: *Thylacosmilus* was not a marsupial "saber-tooth predator". *PeerJ, 8,* e9346.

Jolliffe, I. T., & Cadima, J. (2016). Principal component analysis: a review and recent developments. *Philosophical Transactions of the Royal Society A: Mathematical, Physical and Engineering Sciences, 374*(2065), 20150202. https://doi.org/10.1098/rsta.2015.0202

Kästner, S. B. R. (2014). Anesthesia and analgesia for general surgery. In S. J. Langley-Hobbs, J. L. Demetriou, & J. F. Ladlow (Eds.), *Feline soft tissue and general* *surgery* (pp. 15–27). W.B. Saunders. https://doi.org/10.1016/B978-0-7020-4336-9.00002-0

Kay, R. F., & Cartmill, M. (1977). Cranial morphology and adaptations of *Palaechthon nacimienti* and other paromomyidae (Plesiadapoidea, ?Primates), with a description of a new genus and species. *Journal of Human Evolution*, *6*(1), 19–53. https://doi.org/10.1016/S0047-2484(77)80040-7

Luckett, W. P. (1993). An ontogenetic assessment of dental homologies in therian mammals. In F. S. Szalay, M. J. Novacek, & M. C. McKenna (Eds.). *Mammal phylogeny: Mesozoic differentiation, multituberculates, monotremes, early therians, and marsupials* (pp. 182−204). Springer-Verlag.

Luo, Z.-X. (2007). Transformation and diversification in early mammal evolution. *Nature, 450*(7172), 1011–1019. https://doi.org/10.1038/nature06277

Mackinnon, S. E., & Dellon, A. L. (1995). Fascicular patterns of the hypoglossal nerve. *Journal of Reconstructive Microsurgery, 11*(3), 195–198. https://doi.org/10.1055/s-2007-1006531

Macrini, T. E. (2006). *The evolution of endocranial space in mammals and non-mammalian cynodonts* (Doctoral Dissertation, University of Texas at Austin). Available from http://hdl.handle.net/2152/13066

Macrini, T. E., Rowe, T., & VandeBerg, J. L. (2007). Cranial endocasts from a growth series of *Monodelphis domestica* (Didelphidae, Marsupialia): a study of individual and ontogenetic variation. *Journal of Morphology, 268*(10), 844–865. https://doi.org/10.1002/jmor.10556

Marshall, L. G. (1976). Evolution of the Thylacosmilidae, extinct saber-tooth marsupials of South America. *PaleoBios, 23,* 1–30.

Milne, A. O., Muchlinski, M. N., Orton, L. D., Sullivan, M. S., & Grant, R. A. (2021). Comparing vibrissal morphology and infraorbital foramen area in pinnipeds. *The Anatomical Record, 305*(3), 556–567. https://doi.org/10.1002/ar.24683

Mitchinson, B., Grant, R. A., Arkley, K., Rankov, V., Perkon, I., & Prescott, T. J. (2011). Active vibrissal sensing in rodents and marsupials. *Philosophical Transactions of the Royal Society B: Biological Sciences, 366*(1581), 3037–3048. https://doi.org/10.1098/rstb.2011.0156

Moehlman, P. D., & Hayssen, V. (2018). *Canis aureus* (Carnivore: Canidae). *Mammalian Species, 50*(957), 14–25. https://doi.org/10.1093/mspecies/sey002

Muchlinski, M. N. (2008). The relationship between the infraorbital foramen, infraorbital nerve, and maxillary mechanoreception: implications for interpreting the paleoecology of fossil mammals based on infraorbital foramen size. *The Anatomical Record, 291*(10), 1221–1226. https://doi.org/10.1002/ar.20742

Muchlinski, M. N. (2010a). Ecological correlates of infraorbital foramen area in primates. *American Journal of Physical Anthropology, 141*(1), 131–141. https://doi.org/10.1002/ajpa.21137

Muchlinski, M. N. (2010b). A comparative analysis of vibrissa count and infraorbital foramen area in primates and other mammals. *Journal of Human Evolution, 58*(6), 447–473. https://doi.org/10.1016/j.jhevol.2010.01.012

Muchlinski, M. N., Wible, J. R., Corfe, I., Sullivan, M., & Grant, R. A. (2020). Good vibrations: The evolution of whisking in small mammals. *The Anatomical Record, 303*(1), 89–99. https://doi.org/10.1002/ar.23989

O'Leary, M. A., Bloch, J. I., Flynn, J. J., Gaudin, T. J., Giallombardo, A., Giannini, N. P., Goldberg, S. L. *et al*. (2013). The placental mammal ancestor and the post–K-Pg radiation of placentals. *Science, 339*(6120), 662–667.

Nelson, A., Engelman, R. K., & Croft, D. A. (2023). How to weigh a fossil mammal? South American notoungulates as a case study for estimating body mass in extinct clades. *Journal of Mammalian Evolution*, *30*, 773–809. https://doi.org/10.1007/s10914-023-09669-1

Patrizi, G., & Munger, B. L. (1966). The ultrastructure and innervation of rat vibrissae. *Journal of Comparative Neurology*, *126*(3), 423–435. https://doi.org/10.1002/cne.901260305

Prevosti, F. J., Forasiepi, A. M., Ercoli, M. D., & Turazzini, G. F. (2012). Paleoecology of the mammalian carnivores (Metatheria, Sparassodonta) of the Santa Cruz Formation. In: Vizcaíno S.F., Kay R.F. & Bargo M.S. (Eds), *Early Miocene paleobiology in Patagonia: high-latitude paleocommunities of the Santa Cruz Formation* (pp. 173–193). Cambridge University Press.

Rieger, I. (1981). *Hyaena hyaena*. *Mammalian Species*, *150*, 1–5. https://doi.org/10.2307/41353899

Riggs, E. S. (1933). Preliminary description of a new marsupial saber-tooth from the Pliocene of Argentina. *Field Museum of Natural History, Geological Series*, *6*, 61–66.

Riggs, E. S. (1934). A new marsupial saber-tooth from the Pliocene of Argentina and its relationships to other South American predaceous marsupials. *Transactions of the American Philosophical Society, New Series, 24*(1), 1–32. https://doi.org/10.2307/3231954

Sánchez-Villagra, M. R., & Asher, R. J. (2002). Cranio-sensory adaptations in small faunivorous semiaquatic mammals, with special reference to olfaction and the trigeminal system. *Mammalia, 66*(1), 93–110. https://doi.org/10.1515/mamm.2002.66.1.93

Schneider, C. A., Rasband, W. S., & Eliceiri, K. W. (2012). NIH Image to ImageJ: 25 years of image analysis. *Nature Methods*, *9*, 671–675. https://doi.org/10.1038/nmeth.2089

Standring, S. (Ed.). (2016). *Gray's anatomy: The anatomical basis of clinical practice* (41st ed.). Elsevier Limited. https://www.clinicalkey.com/dura/browse/bookChapter/3-s2.0-C20110053139

Suarez, C., Forasiepi, A. M., Babot, M. J., Shinmura, T., Luque, J., Vanegas, R. D., *et al*. (2023). A sabre-tooth predator from the Neotropics: Cranial morphology of *Anachlysictis gracilis* Goin, 1997 (Metatheria, Thylacosmilidae), based on new specimens from La Venta (Middle Miocene, Colombia). *Geodiversitas*, *45*(18), 497–572.

Van Valkenburgh, B. (1990). Skeletal and dental predictors of body mass in carnivores. In J. Damuth & B. J. MacFadden (Eds.), *Body size in mammalian paleobiology estimation and biological implications* (pp. 181–205). Cambridge University Press. https://cir.nii.ac.jp/crid/1573950398851008640

Voss, R.S., & S.A. Jansa. 2009. Phylogenetic relationships and classification of didelphid marsupials, an extant radiation of New World metatherian mammals. *Bulletin of the American Museum of Natural History*, *322,* 1–177.

Wible, J. R. (2003). On the cranial osteology of the short-tailed opossum *Monodelphis brevicaudata* (Didelphidae, Marsupialia). *Annals of Carnegie Museum*, *72*(3), 137–202.

Wilson, G. P., Evans, A. R., Corfe, I. J., Smits, P. D., Fortelius, M., & Jernvall, J. (2012). Adaptive radiation of multituberculate mammals before the extinction of dinosaurs. *Nature*, *483*(7390), 457–460. https://doi.org/10.1038/nature10880

Wroe, S., & Sansalone, G. (2023). Marsupial functional morphology, biomechanics, and feeding ecology. In N. C. Caceres & C. R. Dickman (Eds.), *American and Australasian Marsupials* (pp. 1–30). Springer Nature. https://doi.org/10.1007/978-3-030-88800-8_40-1

Wroe, S., Chamoli, U., Parr, W. C. H., Clausen, P., Ridgely, R., & Witmer, L. (2013). Comparative biomechanical modeling of metatherian and placental sabertooths: A different kind of bite for an extreme pouched predator. *PLoS One, 8*, e66888. https://doi.org/10.1371/journal.pone.0066888

Zimicz, A. N. (2012). *Ecomorfología de los marsupiales paleógenos de América del Sur* (doctoral dissertation, Universidad Nacional de La Plata). Available from https://doi.org/10.35537/10915/29337

Figure captions

Figure 1. Methodology used to measure the infraorbital foramen area using CT-scans (see Methods). **1,** section with the coronal plane (red) perpendicular to the infraorbital canal at the level of the infraorbital foramen; **2,** section with the axial plane (green) parallel to the main axis of the infraorbital canal; **3,** section with the sagittal plane (yellow) parallel to the main axis of the infraorbital canal; **4,** general view of a 3D model of a cranium showing the orientation of the planes; **5,** same as 4 with the cranium in transparency and the infraorbital canal in blue.

Figure 2. XY plot graphics contrasting natural logarithms (ln) of: **1,** infraorbital foramen area (IOF_{area}) vs. Cranium size (CS; i.e., geometric mean) in Sparassodonta, Marsupialia, and Carnivora (Dataset 1); **2,** foramen rotundum area (FR_{area}) vs. CS in Sparassodonta and selected marsupials (Dataset 3); **3,** IOF_{area} vs. FR_{area} in Sparassodonta and selected marsupials (Dataset 3; see methods).

Figure 3. Rendered views of three-dimensional models of two saber-tooth skulls showing the infraorbital foramen (IOF) for comparative purposes. **1,** *Thylacosmilus atrox* holotype (FMNH P14531); **2,** *Smilodon populator* (MACN-Pv 18057).

TABLES

Table 1. Measurements from CT scans and estimations for Sparassodonta and Didelphidae. Infraorbital foramen (IOF_{area}) and foramen rotundum (FR_{area}) areas are shown in mm^2. Body mass (BM) was estimated through equations (Eq.) based on: (1) orbital occiput length (Van Valkenburgh, 1990); and (2) M2 length (Zimicz,2012). The cranium size (CS = geometric mean) and relative IOF_{area} follow Muchlinski (2010b).

SUPPLEMENTARY ONLINE INFORMATION

Supplementary Figures.

Supplementary Tables.

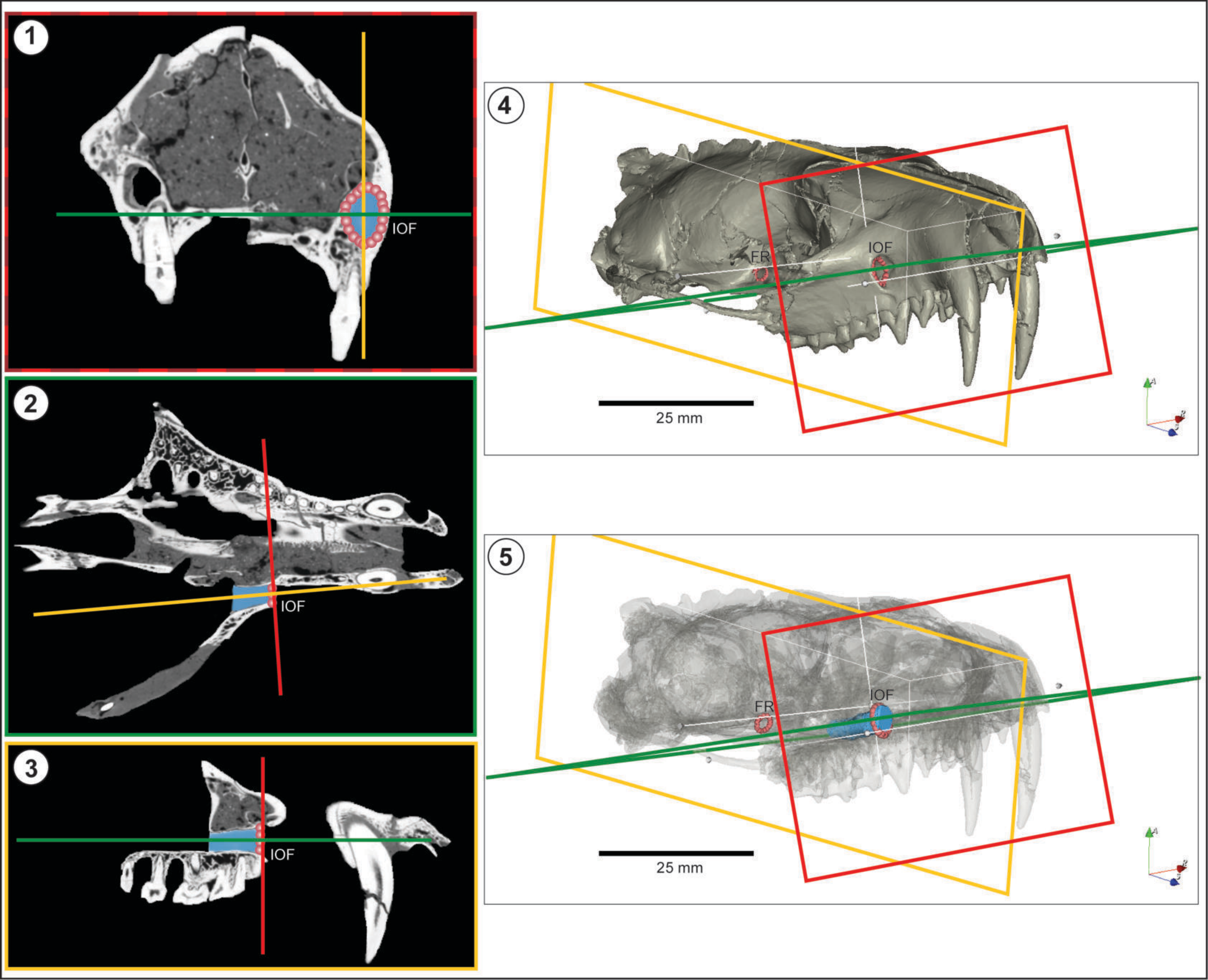
1
IOF
2
IOF
3
IOF
4
FR
IOF
25 mm
5
FR
IOF
25 mm

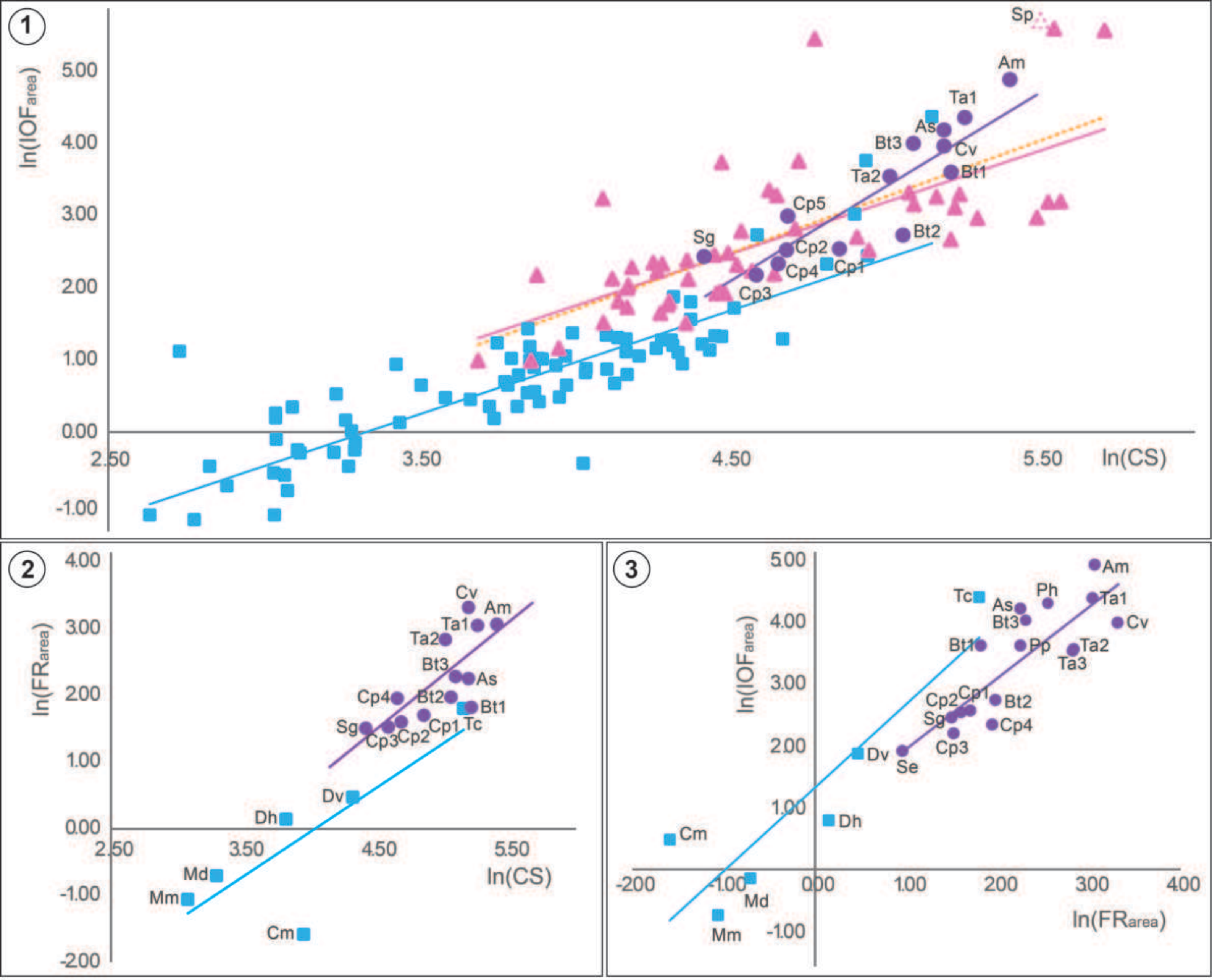

TAXONOMIC ABBREVIATIONS

Am *Arctodictis munizi* CORDPZ121
As *Arctodictis sinclairi* MLP-PV 85-VII-3-1
Bt1 *Borhyaena tuberata* MPM-PV 4380
Bt2 *Borhyaena tuberata* MPM-PV 3625
Bt3 *Borhyaena tuberata* YPM-VPPU 15120
Cv *Callistoe vincei* PVL 4187
Cp1 *Cladosictis patagonica* MACN-A 5927
Cp2 *Cladosictis patagonica* MPM-PV 3645
Cp3 *Cladosictis patagonica* MPM-PV 4323
Cp4 *Cladosictis patagonica* MPM-PV 4326
Cp5 *Cladosictis patagonica* YPM-VPPU 15170
Ph *Pharsophorus* sp. MCNAM-PV 4957
Pp *Prothylacynus patagonicus* YPM-VPPU 15700
Se *Sipalocyon externus* MACN-Pv CH1911
Sg *Sipalocyon gracilis* AMNH-VP 9254
Sp *Smilodon populator* MACN-Pv 18057
Ta1 *Thylacosmilus atrox* FMNH P14531
Ta2 *Thylacosmilus atrox* MMP 1443-M
Ta3 *Thylacosmilus atrox* MLP-PV 35-X-4-1

Cm *Chironectes minimus* MACN-Ma 24300
Dh *Dasyurus hallucatus* TMM M-6921
Dv *Didelphis virginiana* TMM M-2517
Md *Monodelphis domestica* AMNH 261241
Mm *Marmosa murina* NMB 5014
Tc *Thylacinus cynocephalus* NMB c.2526

REGRESSIONS

Line	Equation	R^2
1. Sparassodonta	$\ln(IOF_{area}) = 2.6153 \ln(CS) - 9.6510$	0.7966
Marsupialia	$\ln(IOF_{area}) = 1.4340 \ln(CS) - 4.7060$	0.7175
Carnivora	$\ln(IOF_{area}) = 1.4338 \ln(CS) - 4.0080$	0.5121
Carnivora+Sparass.	$\ln(IOF_{area}) = 0.6810 \ln(CS) - 0.4400$	0.5643
2. Sparassodonta	$\ln(FR_{area}) = 1.5989 \ln(CS) - 5.7334$	0.5707
Marsupialia	$\ln(FR_{area}) = 1.3232 \ln(CS) - 5.3663$	0.6532
3. Sparassodonta	$\ln(IOF_{area}) = 1.1399 \ln(FR_{area}) + 0.8166$	0.6948
Marsupialia	$\ln(IOF_{area}) = 1.3406 \ln(FR_{area}) + 1.3181$	0.8029

Marsupialia
Sparassodonta
Carnivora+Sparassodonta
Carnivora
Smilodon populator

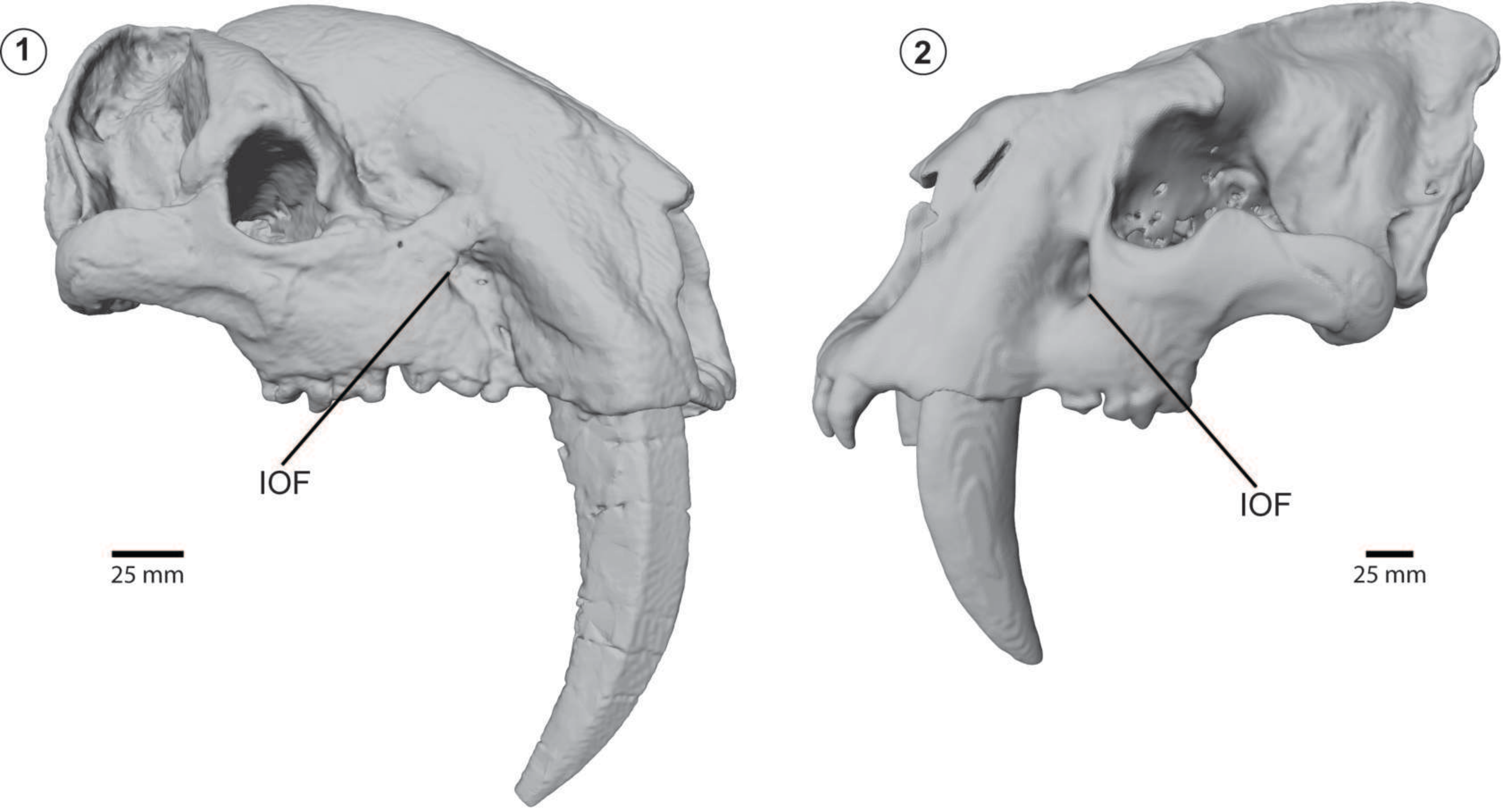
1
IOF
25 mm
2
IOF
25 mm

TABLE 1. Measurements from CT scans and estimations for Sparassodonta and Didelphidae. Infraorbital foramen (IOF_{area}) and foramen rotundum (FR_{area}) areas are shown in mm^2. Body mass (BM) was estimated through equations (Eq.) based on: (1) orbital occiput length (Van Valkenburgh, 1990); and (2) M2 length (Zimicz, 2012). The cranium size (CS = geometric mean) and relative IOF_{area} follow Muchlinski (2010b).

Species	Specimen	IOF_{area}	FR_{area}	FR_{area}/IOF_{area}	CS	Relative IOF_{area}	BM (kg)	Eq.	Olfactory bulbs (%)	Orbital convergence (°)
Arctodictis munizi	CORDPZ121	132.10	21.30	0.16	222.62	1.09	156.01	1	6.70	-
Arctodictis sinclairi	MLP-PV 85-VII-3-1	65.64	9.46	0.14	179.97	1.06	64.78	1	7.80	53.10
Arminiheringia auceta	MACN-A 10970-10972	59.91	-	-	-	-	29.74	2	-	-
Borhyaena tuberata	MPM-PV 3625	15.27	7.18	0.17	157.80	0.85	40.33	1	-	56.60
Borhyaena tuberata	MPM-PV 4380	36.64	6.17	0.47	184.12	0.94	59.82	1	-	58.10
Borhyaena tuberata	YPM-VPPU 15120	54.88	9.88	0.18	163.00	1.07	47.74	1	5.70	-
Callistoe vincei	PVL 4187	52.33	27.50	0.53	179.93	1.01	22.28	2	8.80	-
Cladosictis patagonica	MACN-A 5927	12.64	5.46	0.43	128.52	0.90	6.53	2	4.50	86.10
Cladosictis patagonica	MPM-PV 3645	12.45	4.95	0.40	108.45	0.99	6.72	2	4.10	76.90
Cladosictis patagonica	MPM-PV 4323	8.79	4.56	0.52	98.31	0.96	11.00	1	5.30	49.40
Cladosictis patagonica	MPM-PV 4326	10.26	7.02	0.68	105.51	0.96	5.30	2	3.90	59.40
Cladosictis patagonica	YPM-VPPU 15170	19.88	-	-	108.79	1.09	5.22	2	4.50	-
Patagosmilus goini	MLP-PV 07-VII-1-1	45.46	-	-	-	-	19.79	2	-	-
***Pharsophorus* sp.**	MCNAM-PV 4957	73.25	-	-	-	-	75.07	1	-	-
Prothylacynus patagonicus	MACN-A 5931-5932	-	-	-	130.03	-	25.95	2	5.80	-
Prothylacynus patagonicus	YPM-VPPU 15700	35.96	9.51	0.26	-	-	21.47	2	5.30	-
Sipalocyon externus	MACN-Pv CH1911	6.73	2.62	0.39	-	-	2.27	2	5.80	60.70
Sipalocyon gracilis	AMNH-VP 9254	11.37	4.49	0.39	83.15	1.13	3.06	2	5.80	54.30
Sipalocyon sp.	MPM 4316	5.57	-	-	-	-	2.55	2	5.60	59.50
Thylacosmilus atrox	FMNH P14531	77.88	20.90	0.27	192.55	1.06	69.55	1	3.20	34.80
Thylacosmilus atrox	MMP 1443-M	34.42	16.95	0.49	151.37	1.02	35.11	1	6.40	30.70
Thylacosmilus atrox	MLP-PV 35-X-4-1	33.55	16.90	0.50	-	-	33.87	1	-	-
Chironectes minimus	MACN-Ma 24300	1.63	0.20	0.13	52.09	0.89	0.83	2	4.30	46.80
Dasyurus hallucatus	TMM M-6921	2.21	1.16	0.52	45.65	1.01	0.87	2	8.00	46.60
Didelphis virginiana	TMM M-2517	6.53	1.60	0.25	75.27	1.09	2.86	2	11.00	50.90
Marmosa murina	NMB 5014	0.48	0.35	0.57	21.70	0.87	0.05	2	-	-
Monodelphis domestica	AMNH 261241	0.86	0.49	0.72	27.01	0.95	0.12	2	10.92	43.41
Thylacinus cynocephalus	NMB c.2526	79.44	6.04	0.08	172.97	1.39	20.56	2	6.15	63.80